

Effect of the Interface Roughness on the Elastic Moduli

Tatyana Khachkova[1(✉)], Vadim Lisitsa[2], and Dmitry Kolyukhin[2]

[1] Institute of Petroleum Geology and Geophysics SB RAS, Koptug Avenue 3, Novosibirsk 630090, Russia
khachkovats@ipgg.sbras.ru

[2] Institute of Mathematics SB RAS, Koptug Avenue 4, Novosibirsk 630090, Russia
lisitsavv@ipgg.sbras.ru

Abstract. In this paper, we study the effect of the interface roughness on the elastic parameters of layered media. We consider the three-dimensional models of a layered medium with two different elastic materials inside and outside the layer. We generate the first class of models, where the interfaces between the layers are rough, and the elastic parameters of the inner layers are fixed. Then, the numerical upscaling technique is applied to estimate the effective stiffness tensor. Next, we downscale the stiffness tensor to reconstruct the new elastic parameters of the inner layer for the model of second class with flat interfaces; that is the uncertainty of the model geometry is mapped to the uncertainty of the stiffness tensor component for a fixed geometry of the model. After that, we propose an algorithm for extending the results of restoring the elastic tensors for arbitrary parameters of uncertainty applying the bilinear regression with respect to interface rough parameters and bilinear interpolation using two nearest points with respect to the physical parameters of the inner layers. Verification of the algorithm shows that the errors in the recovering covariance matrix do not exceed 7%; that is, it can be used to statistically simulate models of the second class with a flat interface by arbitrary values of the interface roughness and the physical parameters of the layers in the first class of models.

Keywords: Rough interfaces · Static elastic loading · Upscaling · Statistical analysis

1 Introduction

The construction of continuum mathematical models of physical processes is always based on the consideration of a representative volume in which the change

V. Lisitsa performed numerical simulation using the Supercomputer of the Saint-Petersburg Polytechnical University under the support of Russian Science Foundation grant no. 21-71-20003. D. Kolyukhin generated the models with rough interfaces under the support of Russian Science Foundation grant no. 19-77-20004. T. Khachkova did the statistical analysis of the results.

© The Author(s), under exclusive license to Springer Nature Switzerland AG 2022
O. Gervasi et al. (Eds.): ICCSA 2022 Workshops, LNCS 13378, pp. 328–339, 2022.
https://doi.org/10.1007/978-3-031-10562-3_24

in the considered physical parameters is assumed to be negligible, i.e. volume can be considered homogeneous. Relations between physical parameters on the microscale are replaced by the equations of state implicitly accounting for the macroscopic quantities. To establish these relationships, either the data of laboratory experiments are used, or the problem is solved at the micro level with a subsequent transition to a larger scale (upscaling). As the result, fundamentally different mathematical models can be considered on different scales. An example of problems for which the same mathematical models are used on the micro- and macroscales are the problems of "averaging" or the homogenization of medium models. For example, a rock on the scale of centimeters can be considered as a perfectly elastic body, which, however, is extremely inhomogeneous. At the same time, the characteristic scale of the studied seismic processes is from tens of meters in seismic exploration to tens of kilometers in seismology, which is determined by the characteristic wavelength. In this case, no significant scattering occurs at such small inhomogeneities, and the medium can be considered as a homogeneous ideally elastic medium, but with complex anisotropy. To construct homogenizations for elastic media, both analytical methods [2,3,10] for relatively simple media (periodic structures) and numerical methods based on solving a set of problems in the static theory of elasticity [1,8,9] can be used.

Analytical homogenization methods for layered media have become widespread in exploration seismic [2,4,10], since in the structure of the earth's crust in the absence of tectonic disturbances predominantly there is a weak variability of the parameters of the environment in the horizontal direction in comparison with the vertical one. Therefore, one of the most applicable models in seismic exploration is a model of a vertical transversely isotropic medium as a result of averaging a layered shared with isotropic layers. However, these models are obtained under the assumption that the interfaces between the layers are flat [2,10], which is not always true. The presence of irregularities at the interfaces leads to errors in determining the parameters of effective models, which, in turn, can affect quality of processing and interpretation of seismic data. In our work, we provide a numerical study of the effect of interfaces roughness on the effective elastic parameters of the averaged models. Moreover, the algorithm allows for given roughness parameters to reconstruct models with flat layer boundaries, but allowing fluctuations of elastic parameters in the layer, such that the effective parameters for the original and restored models are the same. Establishing the relationship between the interfaces roughness, which is always outside the resolution seismic methods, and uncertainties in the effective model will significantly increase reliability of seismic data interpretation.

In paper [5] we presented the results of the two-dimensional experiments and the corresponding conclusions. This work considers the three-dimensional case. Since the calculations for such models are much more resource-intensive, the series of experiments were performed in a smaller volume compared to the two-dimensional case, but the results obtained confirm the earlier conclusions.

The paper has the following structure. We formulate the problem in Sect. 2. Numerical experiments are provided in Sect. 3. Statistical modeling the tensors of elastic moduli for the inner layer with using the covariance matrices is presented in Sect. 4.

2 Statement of the Problem

Let's consider static elastic equation stated in a rectangular representative volume $\Omega = [0, X_1] \times [0, X_2] \times [0, X_3]$ written in Cartesian coordinates

$$\begin{gathered}
\frac{\partial}{\partial x_1}\left(c_{11}\frac{\partial u_1}{\partial x_1} + c_{12}\frac{\partial u_2}{\partial x_2} + c_{13}\frac{\partial u_3}{\partial x_3}\right) + \frac{\partial}{\partial x_2}\left(c_{66}\frac{\partial u_1}{\partial x_2} + c_{66}\frac{\partial u_2}{\partial x_1}\right) + \frac{\partial}{\partial x_3}\left(c_{55}\frac{\partial u_1}{\partial x_3} + c_{55}\frac{\partial u_3}{\partial x_1}\right) = 0, \\
\frac{\partial}{\partial x_1}\left(c_{66}\frac{\partial u_2}{\partial x_1} + c_{66}\frac{\partial u_1}{\partial x_2}\right) + \frac{\partial}{\partial x_2}\left(c_{12}\frac{\partial u_1}{\partial x_1} + c_{22}\frac{\partial u_2}{\partial x_2} + c_{23}\frac{\partial u_3}{\partial x_3}\right) + \frac{\partial}{\partial x_3}\left(c_{44}\frac{\partial u_2}{\partial x_3} + c_{44}\frac{\partial u_3}{\partial x_2}\right) = 0, \\
\frac{\partial}{\partial x_1}\left(c_{55}\frac{\partial u_3}{\partial x_1} + c_{55}\frac{\partial u_1}{\partial x_3}\right) + \frac{\partial}{\partial x_2}\left(c_{44}\frac{\partial u_3}{\partial x_2} + c_{44}\frac{\partial u_2}{\partial x_3}\right) + \frac{\partial}{\partial x_3}\left(c_{13}\frac{\partial u_1}{\partial x_1} + c_{23}\frac{\partial u_2}{\partial x_2} + c_{33}\frac{\partial u_3}{\partial x_3}\right) = 0
\end{gathered} \tag{1}$$

with boundary conditions:

$$\begin{gathered}
\sigma_{11}(0, x_2, x_3) = \sigma_{11}^1,\ \sigma_{11}(X_1, x_2, x_3) = \sigma_{11}^1, \\
\sigma_{12}(0, x_2, x_3) = \sigma_{12}^1,\ \sigma_{12}(X_1, x_2, x_3) = \sigma_{12}^1, \\
\sigma_{13}(0, x_2, x_3) = \sigma_{13}^1,\ \sigma_{13}(X_1, x_2, x_3) = \sigma_{13}^1, \\
\sigma_{22}(x_1, 0, x_3) = \sigma_{22}^2,\ \sigma_{22}(x_1, X_2, x_3) = \sigma_{22}^2, \\
\sigma_{12}(x_1, 0, x_3) = \sigma_{12}^2,\ \sigma_{12}(x_1, X_2, x_3) = \sigma_{12}^2, \\
\sigma_{23}(x_1, 0, x_3) = \sigma_{23}^2,\ \sigma_{23}(x_1, X_2, x_3) = \sigma_{23}^2, \\
\sigma_{33}(x_1, x_2, 0) = \sigma_{33}^3,\ \sigma_{33}(x_1, x_2, X_3) = \sigma_{33}^3, \\
\sigma_{13}(x_3, x_2, 0) = \sigma_{13}^3,\ \sigma_{13}(x_1, x_2, X_3) = \sigma_{13}^3, \\
\sigma_{23}(x_3, x_2, 0) = \sigma_{23}^3,\ \sigma_{23}(x_1, x_2, X_3) = \sigma_{23}^3,
\end{gathered} \tag{2}$$

where u_1, u_2 and u_3 are the displacement vector components, σ_{ij} are the stress tensor components and c_{ij} are the components of the stiffness tensor. The stress-stain relation can be written with using Voight notations:

$$\begin{pmatrix} \sigma_{11} \\ \sigma_{22} \\ \sigma_{33} \\ \sigma_{23} \\ \sigma_{13} \\ \sigma_{12} \end{pmatrix} = \begin{pmatrix} c_{11} & c_{12} & c_{13} & & & \\ c_{12} & c_{22} & c_{23} & & 0 & \\ c_{13} & c_{23} & c_{33} & & & \\ & & & c_{44} & & \\ & 0 & & & c_{55} & \\ & & & & & c_{66} \end{pmatrix} \begin{pmatrix} \varepsilon_{11} \\ \varepsilon_{22} \\ \varepsilon_{33} \\ 2\varepsilon_{23} \\ 2\varepsilon_{13} \\ 2\varepsilon_{12} \end{pmatrix}, \tag{3}$$

where the strain tensor components are defined as

$$\varepsilon_{ij} = \frac{1}{2}\left(\frac{\partial u_j}{\partial x_i} + \frac{\partial u_i}{\partial x_j}\right).$$

Here we consider orthotropic media with symmetry axes coinciding with the coordinate axes; that is, the stiffness tensor C is assumed to have a block-diagonal structure, as shown in the Eq. (3).

As before [5] for the stiffness tensor C, which generally depends on spatial coordinates, we determine the constant effective stiffness tensor $\tilde{C}$ relating the volume-averaged stress and strain:

$$< \sigma >_V = \tilde{C} < \varepsilon >_V, \tag{4}$$

where $<>_V$ denote the volume-averaging:

$$< f >_V = V^{-1} \int_V f(x_1, x_2, x_3) dv. \tag{5}$$

The solution of this problem is described in detail by us in paper [5].

Further, for two models with stiffness tensors $C^{(1)}(\vec{x})$ and $C^{(2)}(\vec{x})$, the concept of equivalence is introduced, which means that their effective stiffness tensors coincide: $\tilde{C}^{(1)} = \tilde{C}^{(2)}$.

And for two sets of models, statistical equivalence means the coincidence of the first two moments of the solutions to the upscaling problems for them:

$$\begin{aligned} &< (\tilde{C}^{(1)})_m >_E = < (\tilde{C}^{(2)})_m >_E, \\ &cov\left((\tilde{C}^{(1)})_m\right) = cov\left((\tilde{C}^{(2)})_m\right). \end{aligned} \tag{6}$$

Here $<>_E$ denotes the average value over the statistical realizations ensemble; for tensors and vectors it's considered component-wise mean. And *cov* is the covariance matrix of the stiffness tensor components.

Let's consider a model of a layered medium with two different elastic materials inside and outside the layer. We suggest that the outer material is fixed, these are quartz grains, while the parameters of the inner material can be changed. After that, two sets of models are considered.

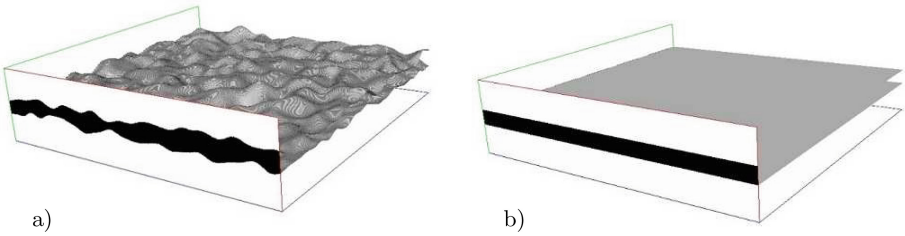

a) b)

Fig. 1. Examples of 3D-models of the layered medium from two types of sets: a) with rough interfaces and constant stiffness tensor of the inner layer; b) with flat interfaces and variable stiffness tensor of the one.

First one are models with rough interfaces and constant elastic moduli of the inner layer (Fig. 1a):

$$C(x_1, x_2, x_3) = \begin{cases} C^f, \, x_3 < b_u(x_1, x_2), \\ C^s, \, b_u(x_1, x_2) \le x_3 \le b_d(x_1, x_2), \\ C^f, \, x_3 > b_d(x_1, x_2), \end{cases} \tag{7}$$

where C^f, C^s are stiffness tensors of first and second layers and interfaces $b_d(x_1, x_2)$ and $b_u(x_1, x_2)$ are random functions:

$$b_d(x_1, x_2) = \langle b_d \rangle + b'_d(x_1, x_2),$$
$$b_u(x_1, x_2) = \langle b_u \rangle + b'_u(x_1, x_2),$$

where mean values $\langle b_u \rangle$, $\langle b_d \rangle$ and inner layer thickness are constant.

Perturbations b'_u and b'_d are random-valued functions with Gaussian probability distribution with zero mean value and covariance function $Q(r)$ defined by the standard deviation φ and correlation length I:

$$Q(r) = \varphi^2 exp(-\frac{\pi r^2}{4I^2}),$$

where r is a separation distance along the interface. For simulation of b'_u and b'_d it's used the method described in [7].

Second set are models with flat interfaces and variable stiffness tensor of the layer (Fig. 1b):

$$\hat{C} = \begin{cases} C^f, \, x_3 < \langle b_u \rangle, \\ \hat{C}^s, \, \langle b_u \rangle \le x_3 \le \langle b_d \rangle, \\ C^f, \, x_3 > \langle b_d \rangle. \end{cases} \tag{8}$$

Here $\hat{C}^s = \left\langle \hat{C}^s \right\rangle + (C^s)'$, where $(C^s)'$ is a random tensor-function with a given covariance matrix.

The main idea of the method is mapping the uncertainty of the model geometry to the uncertainty of stiffness tensor component values for a fixed geometry of the model; that is recovering perturbations of the tensor $\hat{C}^s$ as a function of the roughness of b'_u and b'_d so that two models were statistically equivalent.

The algorithm of equivalent model construction is described in detail in paper [5]. It includes two steps. First, for each model with rough interfaces we apply the numerical upscaling technique to estimate the effective stiffness tensor $\hat{C}$. And then, we downscale the stiffness tensor using formulae Schoenberg [10] to reconstruct the new elastic moduli of the inner layer for the model with flat interfaces [5]. The main question is: how the covariance of the elements of the reconstructed stiffness matrix related to the standard deviation and the correlation length of the interfaces in the original set?

3 Experiments

First, we generate the set of models with rough interfaces (Fig. 1a) using the next parameters: the interlayer thickness is L, the size of model along the layer is $20L$ and the size across the layer is $5L$. The discretization step of the model $h = 0.02L$ was chosen equal in both spatial directions, therefore the discretization of the computational domain was 1000 points along and 250 points across the layer.

As materials outside and inside the layer, we consider an isotropic medium for which the following relations hold $c_{11} = c_{22} = c_{33}$, $c_{44} = c_{55} = c_{66}$ and $c_{12} = c_{13} = c_{23} = c_{11} - 2c_{55}$. Therefore, we define only c_{55} and c_{11} components or c_{11}/c_{55} ratio. For material outside the layer (C^f in Eq. 7) it's used the quartz grains parameters ($c_{11} = 95.4$ GPa, $c_{55} = 44$ GPa), and the different clay parameters $c_{55} \in [6, 16.8, 33]$ GPa, $c_{11}/c_{55} \in [2.17, 3.06, 4]$ GPa are determined for inner layer (C^s in Eq. 7). To simulate rough interfaces at the top and bottom of the inner layer the different values of next two parameters are defined: the correlation length $I \in [0.1L, 0.2L, 0.4L, 0.8L, 1.6L]$ and the standard deviation $\varphi \in [0.02L, 0.04L, 0.1L, 0.2L]$. Specified interfaces are generated independently.

For each of 180 statistical model $[I_i, \varphi_j, (c_{55})_n, (c_{11}/c_{55})_m]$ we generate a series of 10 realizations, after that upscaling and downscaling technique are performed for each such implementation. Finally, the sets of reconstructed stiffness tensors are obtained for interlayers of the equivalent models with flat interfaces (Fig. 1b).

The first characteristic of the obtained tensors, which we investigate, is the component mean calculated over the ensemble of realizations for each statistical models. Since the average layer thickness in the original models is fixed and we keep the same thickness for models of second type, then it's expected that the mean values of the reconstructed tensors coincide with the initial tensors for inner layer. Having calculated the mean values of the tensor components and their confidence intervals, we estimated the relative error between the obtained mean and the tensor, which corresponds to the original model, using the Frobenius norm. Comparison of the obtained relative differences with the norms of relative confidence intervals, which are calculated using the t-distribution, confirms the expected coincidence (Fig. 2). The confidence interval in this case has the form

$$c_{kl} = \bar{c}_{kl} \pm t_{\alpha,N-1} \frac{S}{\sqrt{N}}, \quad S^2 = \frac{\sum_{i=1}^{N} (c_{kl})_i^2 - N\bar{c_{kl}}^2}{N-1}, \tag{9}$$

where $\bar{c}_{kl}$ is mean, S is the variance, N is the size of realizations sample, $t_{\alpha,N-1}$ is a quantile of Student's distribution of level $1 - \alpha/2$ with $N - 1$ degree of freedom, the significance level is chosen as $\alpha = 0.05$.

Then, to check out that the components of the reconstructed stiffness tensors are normally distributed, the Royston's test [6] was used, which confirmed the multivariate normal distribution of the tensor components. Therefore, this distribution is completely determined by the mean vector and the covariance matrix.

So, we have obtained the values of the restored elastic moduli at the points of the regular sparse mesh in four-dimensional parametric space. Further, we propose a method for extending the results to the entire domain of interest, which makes it possible to construct tensors of elastic moduli of the inner layer for arbitrary values of the specified parameters using the covariance matrices.

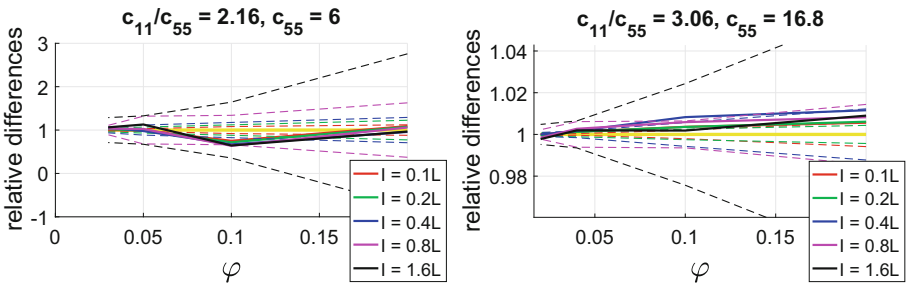

Fig. 2. The relative differences (solid lines) between the original model and mean tensors depending on the standard deviation φ and the correlation length I of rough interface, the dashed lines represent the norms of relative confidence intervals.

4 Interpolation of the Covariance Matrices

The covariance matrices are symmetric and strictly positive definite. Since their size in 3D case is 9×9, then we can apply any explicit method of linear algebra. Let's consider the following interpolation:

$$\Sigma(t) = \exp\left[(1-t)\ln(\Sigma_1) + t\ln(\Sigma_2)\right], \tag{10}$$

where Σ_1 and Σ_2 are the covariance matrices in the point of mesh, and exp and ln are the matrix functions that can be defined as

$$f(\Sigma) = U f(D) U^*,$$

where f is the function (exp or ln), U is the eigenvectors matrix, D is the diagonal matrix whose main diagonal consists of the eigenvalues of Σ, and U^* is conjugate of U. Since the matrix Σ is symmetric, then D is diagonal and real, U is orthogonal and $f(\Sigma)$ is symmetric. And since the functions of the logarithm and exponent are monotonic, then the interpolated matrix is positive.

In order to consider the element-wise representation of the $\Psi = \ln(\Sigma)$ matrices, we fix three of the four parameters and examine the components of Ψ as a function of the remaining parameters (Fig. 3 and 4). We have obtained that the coefficients of the matrices almost linearly depend on $\ln(\varphi)$ and $\ln(I)$, in while the dependence on the physical parameters of the inner layer is more complex.

Next, we calculated a component-wise linear regression of the matrices for each parameter, while the other three parameters were fixed, and considered the relative error of such regression, which is the solution of the equations system by the least-squares method:

$$A_0 y_j + A_1 = \Psi(y_j).$$

Here y is the parameter by which the linear regression is constructed, y_j are its known values, matrices A_0 and A_1 are the coefficients of regression that don't

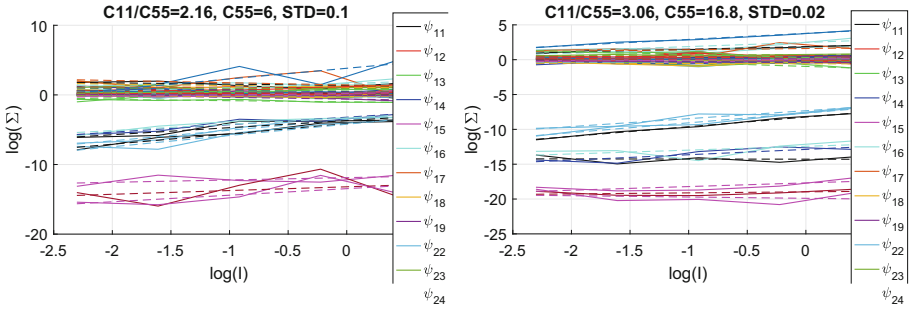

Fig. 3. The components of the matrices $\ln(\Sigma)$ depending on the correlation length I of rough interface for different values of c_{11}, c_{55} and φ. Solid lines correspond to the matrix components; dashed lines are the linear regression of the corresponding components.

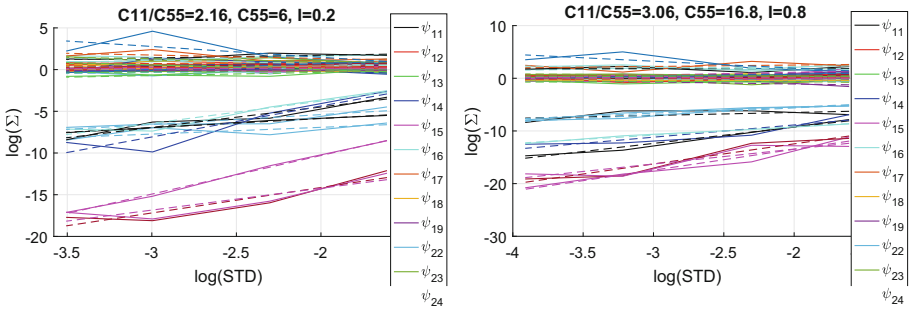

Fig. 4. The components of the matrices $\ln(\Sigma)$ depending on the standard deviation φ of rough interface for different values of c_{11}, c_{55} and I. Solid lines correspond to the matrix components; dashed lines are the linear regression of the corresponding components.

dependent on y. It should be noted that the problem is overdetermined, and it is possible to find a least-squares solution that minimizes the residual:

$$\sum_{ij}\sum_{k}((A_0)_{ij}y_k + (A_1)_{ij} - \psi_{ij}(y_k))^2 = \sum_{k}\|A_0y_k + A_1 - \Psi(y_k)\|_F^2 \to \min.$$

Here $\|\|_F$ is a Frobenius norm

$$\|\Psi\|_F^2 = \sum_{ij}\psi_{ij}^2.$$

For the fixed physical parameters of the inner layer $(c_{11}/c_{55})_m, (c_{55})_n$, we compute the linear regression with respect to I for each φ_j:

$$\hat{\Psi}_{ijmn} = \hat{\Psi}((c_{11}/c_{55})_m, (c_{55})_n, \varphi_j, I)$$
$$= A_0((c_{11}/c_{55})_m, (c_{55})_n, \varphi_j)I + A_1((c_{11}/c_{55})_m, (c_{55})_n, \varphi),$$

then calculate its value at the nodes $I = I_i$ and estimate the relative error as:

$$R_{ijmn} = \frac{\|\hat{\Psi}_{ijmn} - \Psi_{ijmn}\|_F}{\|\Psi_{ijmn}\|_F}.$$

Here Ψ_{ijmn} is the available matrices $\ln(\Sigma)$ at the quadruplets nodes. In Fig. 5 we represent the calculated relative errors depending on the experiment number $M = 5(j-1) + i$, where $j = 1, ...4$, and $i = 1, ...5$. In contrast to the two-dimensional case, where the relative error with respect to the correlation length I did not exceed 0.05, in 3D case the relative errors are larger, reaching 0.15–0.18.

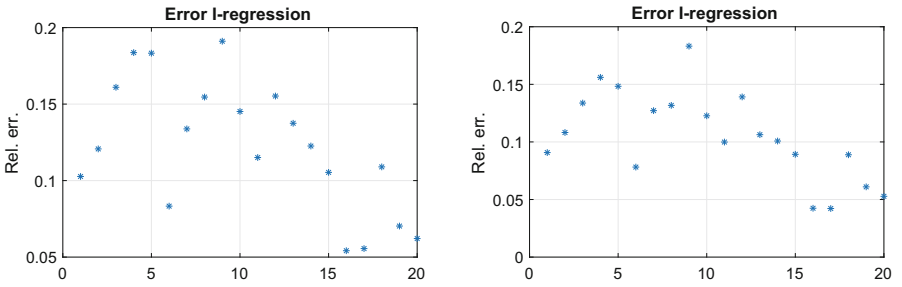

Fig. 5. Relative errors of the linear regression with respect to the correlation length depending on the experiment number at fixed values of the physical parameters $c_{11}/c_{55} = 2.16, c_{55} = 6$ (left) and $c_{11}/c_{55} = 3.06, c_{55} = 16.8$ (right).

Then, similarly, we calculated the relative errors of the linear regression with respect to the standard deviation φ. The results are represented in Fig. 6.

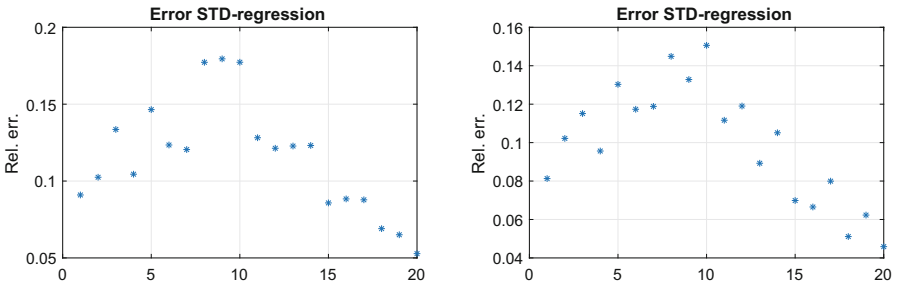

Fig. 6. Relative errors of the linear regression with respect to the standard deviation depending on the experiment number at fixed values of the physical parameters $c_{11}/c_{55} = 2.16, c_{55} = 6$ (left) and $c_{11}/c_{55} = 3.06, c_{55} = 16.8$ (right).

It should be noted that in the Figs. 5 and 6 every five experiments correspond to a fixed standard deviation $\varphi \in [0.2L, 0.1L, 0.04L, 0.02L]$. The first five correspond to $\varphi = 0.2L$ and so on. It can be seen that the relative error decreases

with the standard deviation decrease. And within each five experiments, the correlation length grows, $I \in [0.1L, 0.2L, 0.4L, 0.8L, 1.6L]$. These graphs (Figs. 5 and 6) confirm that the matrix ($\Psi = \ln(\Sigma)$) components are linearly dependent on the functions $\ln(\varphi)$ and $\ln(I)$.

Accordingly, for each pair $((c_{11}/c_{55})_m, (c_{55})_n)$ it can be calculated the bilinear regression; that is, the approximation of Ψ can be founded as:

$$\begin{aligned} \tilde{\Psi}_{mn} &= \tilde{\Psi}((c_{11}/c_{55})_m, (c_{55})_n, \varphi, I) \\ &= B^{11}_{mn}\varphi I + B^{10}_{mn}\varphi + B^{01}_{mn} I + B^{00}_{mn}, \end{aligned} \tag{11}$$

where matrices B^{11}_{mn}, ..., B^{00}_{mn} depend on the parameters $((c_{11}/c_{55})_m, (c_{55})_n)$.

Using the technique described above, we calculate the relative errors for bilinear regression (Fig. 7), which, just like in the case of linear regression, decrease along with a decrease in the standard deviation.

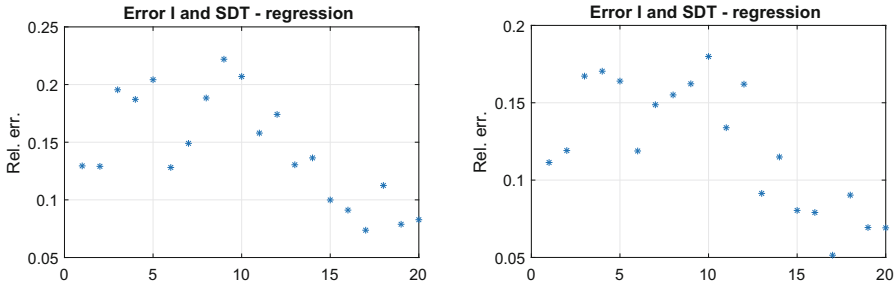

Fig. 7. Relative errors of the bilinear regression depending on the experiment number at fixed values of the physical parameters $c_{11}/c_{55} = 2.16, c_{55} = 6$ (left) and $c_{11}/c_{55} = 3.06, c_{55} = 16.8$ (right).

Since the dependence on the physical parameters of the inner layer is more complex, another interpolation method is needed to restore the values between them. We use standard linear component-wise interpolation with using two nearest points, that is described in detail by us in paper [5].

So, applying the bilinear regression with respect to $\ln(I)$ and $\ln(\varphi)$ and bilinear interpolation using two nearest points with respect to the physical parameters, we reconstruct the covariance matrix at arbitrary point of four-dimensional parametric space.

To test the algorithm for recovering the covariance matrix, we created 18 data sets, each containing 10 realizations, for random quadruples. After calculating the covariance matrices for these datasets, we compared them with the values predicted by the algorithm. In the Fig. 8, we represent the relative errors of the reconstructed matrices Ψ compared to those obtained from numerical experiments using the Frobenius norm. The left plot show the errors depending on the experiment number, the right are the errors depending on the position of input parameters (I, φ).

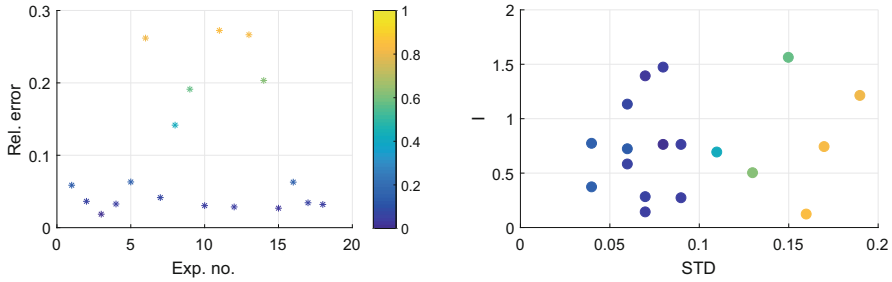

Fig. 8. Relative errors of the recovered matrices Ψ for random quadruplets. Markers colour correspond to the value of error. (Color figure online)

It can be seen that the matrix reconstruction error increases with the growth of the standard deviation φ of rough interface and is independent of the correlation length I. In addition, it can be seen that for the standard deviation $\varphi \in [0.02L, 0.04L, 0.1L, 0.2L]$ only the interval $\varphi \in [0.1L, 0.2L]$ leads to large errors, while for standard deviation values from 0.02L to 0.1L, the errors in recovering the covariance matrix do not exceed 0.07. Thus, with the specified limitation on standard deviation values, the recovery algorithm can be used to statistically simulate models with a flat interface and random material in the inner layer.

5 Conclusions

In this paper, we research the effect of uncertainty of the model geometry on the elastic parameters of the layered media. We consider the three-dimensional models of a layered medium with two different elastic materials inside and outside the layer. Initially, we generate the first class of models, where the interfaces between the layers are rough, and the elastic parameters of the inner layers are fixed. Such models are constructed for different values of parameters at the points of the regular sparse mesh in four-dimensional parametric space. The varied parameters are standard deviation and correlation length of interface roughness and two physical parameters (components of stiffness tensor) of the inner layer. Then, for each model the numerical upscaling technique is applied to estimate the effective stiffness tensor. After that, we downscale the stiffness tensor to reconstruct the new elastic parameters of the inner layer for the model of second class with flat interfaces that is equivalent to original; that is their effective stiffness tensors are coincide.

The next step is investigation of the characteristic of the obtained stiffness tensors, that confirm the coincidence of the mean values of the reconstructed tensor (over the ensemble of realizations) and the initial tensors for inner layer in first models. Since Royston's test confirmed the multivariate normal distribution of the tensor components, and this distribution is completely determined by the mean vector and the covariance matrix, we use this matrix to extend the results

to the entire domain of four-dimensional parametric space; that is we propose the algorithm to reconstruct the stiffness tensors of the inner layer with flat interfaces for arbitrary values of the interface roughness and the physical parameters of the inner layer in the first class of models.

We apply the bilinear regression with respect to interface rough parameters and bilinear interpolation using two nearest points with respect to the physical parameters of the inner layers. So, we reconstruct the covariance matrix at arbitrary point of four-dimensional parametric space. Verification of the algorithm shows that the errors in the recovering covariance matrix do not exceed 7%. Thus, with the specified limitation on standard deviation values, the proposed algorithm can be used to statistically simulate models of the second class with a flat interface by given parameters of uncertainty for the inner layer in the first class of models.

References

1. Andra, H., et al.: Digital rock physics benchmarks - part II: computing effective properties. Comput. Geosci. **50**, 33–43 (2013)
2. Backus, G.E.: Long-wave elastic anisotropy produced by horizontal layering. J. Geophys. Res. **67**(11), 4427–4440 (1962)
3. Capdeville, Y., Guillot, L., Marigo, J.J.: 2-D non-periodic homogenization to upscale elastic media for P–SV-waves. Geophys. J. Int. **182**(2), 903–922 (2010). https://doi.org/10.1111/j.1365-246X.2010.04636.x
4. Henriques, J.P., et al.: Experimental verification of effective anisotropic crack theories in variable crack aspect ratio medium. Geophys. Prospect. **66**(1), 141–156 (2018)
5. Khachkova, T., Lisitsa, V., Kolyukhin, D., Reshetova, G.: Influence of interfaces roughness on elastic properties of layered media. Probab. Eng. Mech. **66**, 103170 (2021)
6. Royston, J.P.: Some techniques for assessing multivarate normality based on the Shapiro-Wilk w. J. R. Stat. Soc. Ser. C (Appl. Stat.) **32**(2), 121–133 (1983)
7. Sabelfeld, K.K.: Monte Carlo Methods in Boundary Value Problems. Springer, Cham (1991)
8. Saenger, E.H.: Numerical methods to determine effective elastic properties. Int. J. Eng. Sci. **46**(6), 598–605 (2008)
9. Saenger, E.H., et al.: Analysis of high-resolution X-ray computed tomography images of Bentheim sandstone under elevated confining pressures. Geophys. Prospect. **64**(4), 848–859 (2016)
10. Schoenberg, M., Muir, F.: A calculus for finely layered anisotropic media. Geophysics **54**(5), 581–589 (1989)